The Journal of National Chiao Tung University
Vol. 3, September 1977
pp. 13-26

空乏區寬度之調變效應對高低高雙飄帶衝度二極體之影響

Effects of Depletion-Region-Width Modulation on the Properties of Lo-Hi-Lo Double Drift IMPATT Diodes

張懋中，陳茂傑 Mau-Chung Chang and Mao-Chieh Chen

The Institute of Electronics, N. C. T. U.

(Received June 10, 1977)

Abstract — The effect of the depletion-region-width modulation has been included in the Quasi-static large signal calculations of the Lo-Hi-Lo double-drift IMPATT diodes. In addition, a linear-generation-function model is introduced to give a comprehensive understanding of the phase advance and the power degradation effect of the diodes. The phase advance $\Delta\phi$ is derived versus of voltage modulation. The output power losses are also calculated as a function of voltage swing and compared with the uncorrected results. Efficiency as a function of avalanche-to drift-voltage ratio V_a/V_d is obtained and $V_a/V_d \approx 1.0$ is shown as the optimum condition for a double drift Lo-Hi-Lo diodes at 50% modulation.

I. Introduction

By synthesizing the numerical technique of Blue's [1] with the quasi-static formulation developed by Kuvås and Lee [2], Decker [3] has accomplished a closed form expressions for the quasi-static approximation and applied it to the calculation of single-sided IMPATT diodes with arbitrary doping profile. However, the model considered in his work didn't include any dynamic modification about the effect of moving edges of the depletion zone, nor the variation of series resistance with the r.f. swing voltage.

This paper presented here basically follows that developed by Decker, but extends its application to cover the double-drift diodes with both kinds of transport carriers (electrons and holes) to increase the power generation of the diode. In addition, the above mentioned dynamic effects, which are indispensable in a strongly modulated condition, has been added to the original model. An efficient and comprehensive linear-generation-function model is introduced to study the effect of phase advance due to zone width modulation, which gives us a deep insight into the dynamic effect comprehensively.

II. Mathematical Analysis

The doping profile of a double drift Lo-Hi-Lo silicon diode is depicted in Fig. 1(a), where X_0 and δ are the depth and width of the buried-layer respectively. Fig. 1(b) shows the electric field distribution for a punched through double-drift Lo-Hi-Lo IMPATT diode at low injection condition and is given by

$$E_1(x)=E_c-\frac{qnx}{\epsilon_s} \qquad 0\le x\le x_0 \qquad (1)$$

$$E_2(x)=E_c+\frac{qpx}{\epsilon_s} \qquad -x_0\le x\le 0 \qquad (2)$$

$$E_3(x)=E_1(x_0)-\frac{qn_b(x-x_0)}{\epsilon_s} \qquad x_0\le x\le x_0+\delta \qquad (3)$$

$$E_4(x)=E_1(-x_0)+\frac{qp_b(x+x_0)}{\epsilon_s} \qquad -(x_0+\delta)\le x\le -x_0 \qquad (4)$$

$$E_5(x)=\frac{qn(W_0-x)}{\epsilon_s} \qquad x_0+\delta \leq x \leq W_0 \tag{5}$$

$$E_6(x)=\frac{qp(W_0+x)}{\epsilon_s} \qquad -W_0 \leq x \leq -(x_0+\delta) \tag{6}$$

where W_0 is the metallurgical depletion width, n & p are the concentrations of the background doping, and n_b & p_b are the concentrations of the buried-layer for each side, respectively. Assuming a symetric double-drift structure, we have n=p and $n_b=p_b$. From equation (1), (3) and (5), the width of the buried layer is found to be

$$\delta = \frac{E_c-\frac{qnW_0}{\epsilon_s}}{\frac{q}{\epsilon_s}(n_b-n)} \tag{7}$$

If n_b is much greater than n, δ is inversely proportional to n_b for a fixed depletion width W_0. In the avalanche zone (Fig. 1(b)), holes move in the positive x-direction, and if the scattering-limited velocity is assumed well saturated under avalanche condition, the time dependent continuity equations for both electrons and holes would take the following forms

$$\frac{\partial i_n}{\partial t}-v_n\frac{\partial i_n}{\partial x}=(\alpha i_n+\beta i_p)v_n \tag{8}$$

$$\frac{\partial i_p}{\partial t}+v_p\frac{\partial i_p}{\partial x}=(\alpha i_n+\beta i_p)v_p \tag{9}$$

where i_n and i_p represent the electron and hole current density respectively, α & β, the ionization rates of electrons and holes respectively, and v_n & v_p, the magnitude of the scattering-limited velocity of electrons and holes respectively. The saturated velocities of electrons and holes had been measured by Canali et. al. [4] at room temperature and higher temperatures. The extrapolation of their data to the 150°C region gives

$V_n=7.56 \times 10^6$ cm/sec, and

$V_p=6.98 \times 10^6$ cm/dec

in the high field approximation. By combining equations (8) and (9) and using a quasi-static approximation, Kuvas and Lee [1] had derived the following salient equations

$$\{\frac{\partial}{\partial t}+(M\tau_i)^{-1}-\lambda[\partial E(t)/\partial t]\}i = \{\tau_i^{-1}-\lambda[\partial E(t)/\partial t]\}i_s \tag{10}$$

$$\tau_i=\kappa\tau \tag{11}$$

$$Mi_s=M_n i_{sn}+M_p i_{sp} \tag{12}$$

$$\left(\frac{i_s}{\tau}\right)=\left(\frac{i_{sn}}{\tau_n}\right)+\left(\frac{i_{sp}}{\tau_p}\right) \tag{13}$$

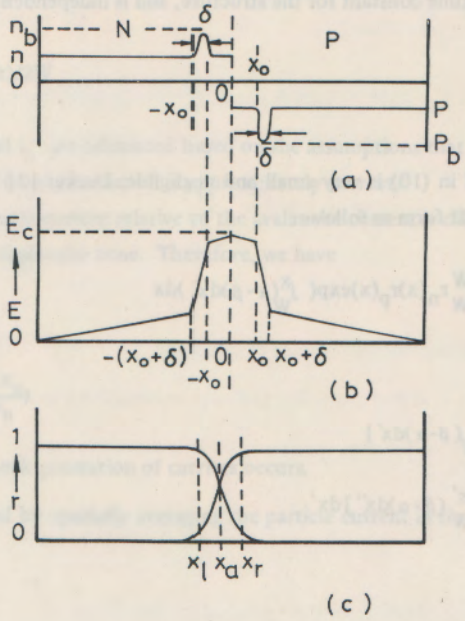

Fig. 1. Double-Drift Lo-Hi-Lo IMPATT diode. The avalanchezone is shifted to the n-side.

where τ is the intrinsic response time, i_s is the total reverse-saturation current of the diode, λ and κ are two parameters, and M_n and M_p are multiplication factors of electron and hole, respectively.

Consider a double-drift IMPATT diode shown in Fig. 1, with a sinusoidal oscillation voltage $V_a=V_{rf}\sin\omega t$ applied to the terminals of the diode. From the Poisson equation the modulated depletion width would be given by

$$W=W_0+\frac{\epsilon_s}{qn}\frac{V_{rf}}{2W}S(t-\frac{T}{2})\sin\omega t \tag{14}$$

where S[t-(T/2)] is defined as a step function and T is the period of the applied voltage. In the first half of the perior, the depletion width should remain in its metallurgical value W_0 and S[t-(T/2)]=0. However, in the second half of the period, W has been modulated, and S[T-(T/2)]=1. The multiplication factor of electron M_n under the modulation field $V_a/2W$ is

$$M_n^{-1}=1-\int_{-W}^{W}\alpha\exp(-\int_{x}^{W}(\alpha-\beta)dx')dx \tag{15}$$

and the corresponding response time is

$$\tau_n=\int_{-W}^{W}\exp(-\int_{x}^{W}(\alpha-\beta)dx')(dx/(v_n+v_p)) \tag{16}$$

These quantities are related to the corresponding values of hole-initiated excitation by

$$M_n/M_p=\tau_p/\tau_n=\exp(\int_{-W}^{W}(\alpha-\beta)dx) \tag{17}$$

Here we note $M_n \tau_n = M_p \tau_p$ as a time constant for the structure, and is independent of whether it is electron or hole excitation, i.e.

$$M_n \tau_n = M_p \tau_p = M\tau \tag{18}$$

Since the parameter λ appeared in (10) is very small and negligible, Decker [3] derived a formula for parameter κ and we extend it to a double-drift form as follows

$$\kappa = \tau_p^{-1}(V_p^{-1}+V_n^{-1}) \int_{-W}^{W} r_n(x) r_p(x) \exp\left(\int_{W}^{x} (\alpha - \beta) dx' \right) dx \tag{19}$$

where

$$r_p(x) = i_p(x)/i = [\exp \int_{-W}^{x} (\beta - \alpha) dx'] \int_{-W}^{x} \alpha(x') \exp[- \int_{W}^{x'} (\beta - \alpha) dx''] dx' \tag{20}$$

and

$$r_n(x) = 1 - r_p(x) = i_n(x)/i \tag{21}$$

From equation (18), the corrected multiplied response time could be derived in terms of equation (19)

$$(M\tau_i)^{-1}(M_n \kappa \tau_n)^{-1} = (M_p \kappa \tau_p)^{-1} = \frac{1 - \int_{-W}^{W} \alpha (\exp \int_{W}^{x'} (\alpha - \beta) dx'') dx'}{(V_n^{-1}+V_p^{-1}) \int_{-W}^{W} r_n(x) r_p(x) (\exp \int_{W}^{x} (\alpha - \beta) dx') dx} \tag{22}$$

In this equation, α and β are functions of the dynamic field E(x,t) and can be approximated in the form [5]:

$$\alpha = A \exp(-B/E) \quad \text{and} \quad \beta = C \exp(-D/E)$$

whereas $r_n(x)$ and $r_p(x)$ are kept at their dc values, and no further modification is made when oscillation voltage is applied. Because the total field is a combination of the dc field, the applied voltage and the space charge feedback due to the drifting carriers, E_t can be written as

$$E_t = (x,t) = E_0(x) + E_a(t) + E_{sc}(x,t) \tag{23}$$

As we know $E_0(x)$ is determined from dc break-down condition for the designed structure and at some specified bias current density. The space-charge induced electric field is given from the Poisson equation and could be shown as

$$E'_{sc}(x,t) = -\frac{1}{\epsilon_s} \int_{x}^{W} \left[\frac{i_p(x',t)}{v_p} - \frac{i_n(x',t)}{v_n} \right] dx' \tag{24}$$

Therefore, when we define the space charge voltage V_{sc} as

$$V_{sc}(t) = \int_{-W}^{W} E'_{sc}(x,t) dx \tag{25}$$

it is necessary to substrate $V_{sc}(t)/2W$ from $E'_{sc}(x,t)$ before adding it to obtain E_t, since the desired terminal voltage

is just the applied voltage, thus

$$E_{sc}(x,t)=E'_{sc}(x,t)-V_{sc}(t)/2W \tag{26}$$

The individual particle current i_p and i_n are calculated based on the assumptions that

(1) the current fraction derived from dc solution is approximately correct:

(2) the phase shift of each particle current relative to the avalanche current is calculated with respect to the total particle current at the center of the avalanche zone. Therefore, we have

$$i_p(x,t)=r_p(x)\cdot i(t-\frac{x-x_a}{v_p}) \tag{27}$$

$$i_n(x,t)=(1-r_p(x))\cdot i(t+\frac{x-x_a}{v_n}) \tag{28}$$

where x_a is the position where the peak generation of carriers occurs.

The external current is calculated by spatially averaging the particle current in the depletion zone and adding to it the displacement current,

$$i_e=i_c+i_d$$

$$=\frac{1}{2W}\{\int_{-W}^{W}(i_p(x',t)+i_n(x',t))dx'+\epsilon_s\frac{dV_a}{dt}\} \tag{29}$$

The first term is the conduction current and the second term the displacement current.

When a sinusoidal perturbation $V_a=V_{rf}\sin\omega t$ is applied to the terminals of an IMPATT diode*, part of the voltage will drop at the under punched-through outlet of the drift zone and dissipate as heat in those regions. Therefore, the voltage which is available to generate the avalanche current is only the remaining part of V_a. With the aid of eq. (14), we obtain this voltage swing $V_g(t)$ as

$$V_g(t)=V_{rf}(1+S(t-\frac{T}{2})\frac{\epsilon_s}{qn}\frac{V_{rf}}{2W^2}\sin\omega t)\cdot\sin\omega t \tag{30}$$

Through Fourier analysis, we have the conductance $G(\omega)$ and the susceptance $B(\omega)$ of the diode as follows

$$G(\omega)=\frac{2}{TV_{rf}}\int_0^T i_c(t).\sin\omega t\,dt \tag{31}$$

$$B(\omega)=\frac{2}{TV_{rf}}\int_0^T i_e(t).\cos\omega t\,dt \tag{32}$$

The r.f. power density radiated in frequency ω is

$$P_{rf}=-\frac{1}{2}V_{rf}^2G(\omega) \tag{33}$$

Power loss resulting in heat dissipation as well as in the form of harmonics due to the zone edges moving is given as

$$P_{loss}=\frac{1}{T}\int_0^T i_e(t)S(t-\frac{T}{2})V_{rf}K\sin^2\omega t\,dt$$

* The diode is supposed to be oscillating with a sinusoidal voltage which is shown impressed across the depletion region.

$$=\frac{1}{2}J_{dc}V_{rf}K\cdot\frac{(V_{rf}K)^2}{8}B(2\omega) \tag{34}$$

where $K=(\epsilon_s/qn)\cdot(V_{rf}/2W^2)$, and J_{dc} is the dc bias current. Generally speaking, the power loss increases with voltage swing but is inversely proportional to the doping concentration of the device. Therefore, the modification seems much important in Lo-Hi-Lo diodes which has a lower background doping concentration compared with the uniformly doped diodes. The power efficiency η is equal to

$$\eta = \frac{P_{rf}}{J_{dc}\cdot V_{dc}} \times 100\% \tag{35}$$

where J_{dc} and V_{dc} are the dc bias current and voltage respectively.

If the small value of parameter λ is negligible, Eq. (10) can be simplified to read

$$[d/dt+(M\tau_i)^{-1}]\, i=i_s/\tau_i \tag{36}$$

From above, i(t) can be solved as

$$i(t)=\exp(-\int_0^t (M\tau_i)^{-1}dt)\cdot\{i(0)+(i_s/\tau_i)\int_0^t dt'\cdot\exp(\int_0^{t'}(M\tau_i)^{-1}dt'')\} \tag{37}$$

The inverse response time $(M\tau_i)^{-1}$ appears as an exponential growth factor for the particle current and under the condition that the total reverse-saturation current is insignificantly small, the particle current is reduced to

$$i(t)=i(0)\cdot\exp(-D(t)) \tag{38}$$

with a generation function D(t):

$$D(t)=\int_0^t (M\tau_i)^{-1}dt \tag{39}$$

Using the numerical procedure similar to that of Blue's, we can solve this system more accurately and more generally. It is not necessary to assume equal drift velocities and ionization rates which are only suitable for certan kinds of semiconductor materials and it is also not necessary to assume a uniform avalanche electric field which exists only in an idealized Read diode.

III. Numerical Considerations

For the sake of clarity, some of the numerical details are omitted in the discussion. First, we adjust static field $E_0(x)$ so that the breakdown condition

$$\int_{-W}^{W}\alpha(E_0)\exp\int_W^{x'}(\alpha(E_0)-\beta(E_0))dx''dx'=1 \tag{40}$$

is fulfilled for a specified diode structure and the desired dc bias current. The depletion width W_0 is determined by the operation frequency $W(\mu)=28/f(GHz)$ for silicon at 150°C [6]. Since the ionization rate of electrons differs from that of holes in silicon at a given temperature, Grant [7] derived a set of equations to fit his experimental data obtained at 150°C as follows

$$\alpha = 1.37\times10^{6}\exp(-1.48\times10^{6}/E)$$

$$\text{for } E < 2.16\times10^{5}\text{V/cm} \tag{41}$$

$$\alpha = 7.52\times10^{5}\exp(-1.35\times10^{6}/E)$$

$$\text{for } E > 2.16\times10^{5}\text{V/cm}$$

for electrons, and

$$\beta = 1.31\times10^{6}\exp(-1.92\times10^{6}/E)$$

$$\text{for } E < 6.07\times10^{5}\text{V/cm}$$

$$\beta = 6.89\times10^{5}\exp(-1.53\times10^{6}/E)$$

$$\text{for } 6.07\times10^{5}\text{V/cm} < E < 6.74\times10^{5}\text{V/cm}$$

$$\beta = 3.28\times10^{5}\exp(-1.03\times10^{6}/E)$$

$$\text{for } E > 6.74\times10^{5}\text{V/cm}$$

for holes.

Since the avalanche oscillators such as IMPATT diodes are operated from constant current power supplies, the dc bias current density J_{dc} is taken as a bias parameter. In order to satisfy a specified bias current, the dc bias voltage V_{dc} has to be corrected from the breakdown value V_B by the relation

$$V_{dc} = V_B \pm (\Delta E_{0p})(2W) \tag{42}$$

where "+" sign is for over punch through and "-" sign for under punch through operations respectively, and $|\Delta E_{0p}|$ is the amount of deviation from the break down field.

A dc solution of the current fraction $r_n(x)$ and $r_p(x)$ are evaluated with Equation (20) and (21). The peak generation position X_a is the position where the magnitude of current gradient

$$\left|\frac{\partial i_n}{\partial x}\right| = \left|\frac{\partial i_p}{\partial x}\right| = (\alpha i_p + \beta i_n) \tag{43}$$

has the maximum value. $r_n(x)$, $r_p(x)$ and X_a derived above are assumed approximately correct in the dynamic electric field case without any further modifications. For an applied voltage $V_a(t)$, the situation may be viewed as an initial-value problem where the response of the diode is determined simply from Equation (38). By properly assuming an initial current i(0), the time evolution of avalanche current i(t) and external induced current $i_c(t)$ could be computed iteratively. Practically, the periodic steady state response $i_c(t)$ with respect to an applied voltage $V_a(t)$, not the transient response from some arbitrary initial state, is of great interest. Therefore, in this work, the time integration is carried out after a steady state has been reached; the transient behavior is not discussed. The total time required to achieve the steady state is typically 10 r.f. periods. Each period is divided into a number of time steps (typically 50). The condition that the current response must be periodic leads to the average value of $(M\tau_i)^{-1}$ over one period equal to zero, namely

$$D(T)= \int_0^T (M\tau_i)^{-1} dt=0 \tag{44}$$

Therefore, after each computation cycle is finished, the n'th run initial current $i^n(0)$ should be replaced by $i^{n-1}(T)$. The procedure continues until a steady solution has been achieved, i.e., for an prescribed infinitesimal value ξ

$$| i^n(T)-i^n(0) | < \xi \tag{45}$$

is satisfied, and the current response for a given driving condition is hereby obtained.

IV. Results And Discussions

Four samples of representative Si diodes (named as A, B, C, and D) are submitted to the modified quasi-static large signal calculations without losing any generality. Dimensions of X_0 and δ of the buried layer are chosen for the convenience of ion implantation (especially the 200 KeV P^+, and 300 KeV B^{++} doping). By varing the doping concentration n(p) and $N_b(p_b)$, the avalanche to drift voltage ratios V_a/V_d are varied from 0.84 to 3.40. Table 1 gives the specification of diodes wherein W_0 is the fixed depletion zone width of single side, X_0 the depth of buried layer, δ the width of buried layer, n the background concentration, n_b the buried-layer concentration V_B the breakdown voltage (biased at J_{dc}=550 A/cm^2), and V_a/V_d the avalanche to drift voltage ratio (also biased at J_{dc}=550 A/cm^2). The single-sided drift length W_0=2.8 was postulated at 10 GHz by a generally accepted formula [6].

Table 1. Specification of Diodes

No.	$W_0(\mu)$	$X_0(\mu)$	$\delta(\mu)$	$n(\frac{1}{cm^3})$	$n_b(\frac{1}{cm^3})$	V_B(volts)	V_a/V_d
A	2.8	0.26	0.16	6×10^{15}	9×10^{16}	82.3	0.84
B	2.8	0.26	0.16	5×10^{15}	11.5×10^{16}	73.5	0.9
C	2.8	0.26	0.16	3×10^{15}	13.5×10^{16}	55.1	1.44
D	2.8	0.26	0.16	9.8×10^{14}	16.7×10^{16}	36.5	3.4

The conductance and susceptance values are shown as an admittance plot in Fig. 2 and Fig. 3. The result of the large signal analysis shows that the optimum bias current at 10 GHz occurs around J_{dc}=550 A/cm^2. The same results can be deduced from the plasma resonance formula $f_r=(1/2\pi)\sqrt{[3\alpha' v_s J_{dv}/\epsilon_s]}$ [8] in combination with the critirion of SG [9] model, that is $f_{op}=1.2\, f_r$.

Output power as a function of rf voltage modulation is shown in Fig. 4 and Fig. 5. The power output is monotonically increasing when the series resistance of the unswept depletion region is ignored. The incorporation of zone width modulation in Eq. (14) reduces the efficienty and causes observable saturation of power output with r.f. drive. An estimate of this power reduction could be derived by introducing a linear-generation-function model, which accounts for the zone modulation effect.

Fig. 6 shows the generation-function $(M\tau_i)^{-1}$ versus electric field [10]. The linear approximation for $(M\tau_i)^{-1}$ around breakdown in shown by dotted line. This approximation makes some error around the minimum of the time dependent E(t). However, the model does give us a comprehensive physical picture concerning the moving zone edges with the phase advance and the output power degradation. The time average $\int_0^T (M\tau_i)^{-1} dt=0$ is a necessary condition in achieving a steady periodic solution for the avalanche diode. Thus, from the linear-generation-function model

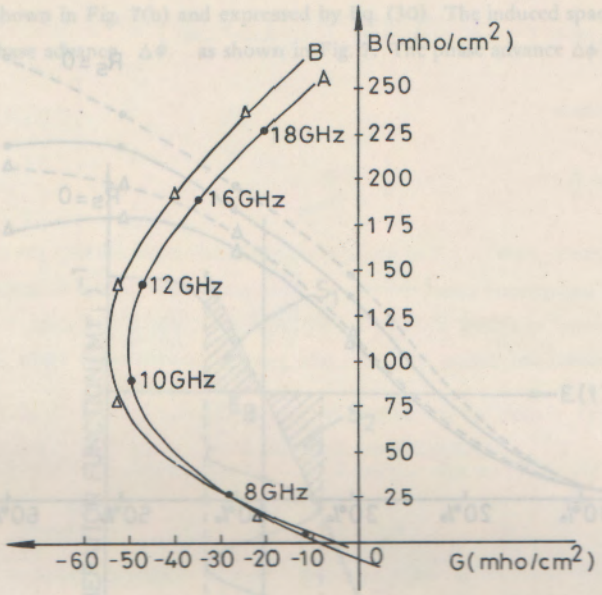

Fig. 2. Admittance diagram for diodes A and B at bias current 550 A/cm^2 with 5% modulation.

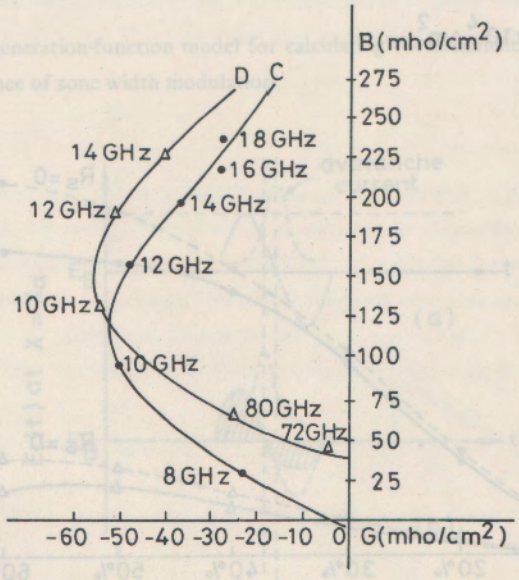

Fig. 3. Admittance diagram for diodes C and D at bias current 550 A/cm^2 with 5% modulation.

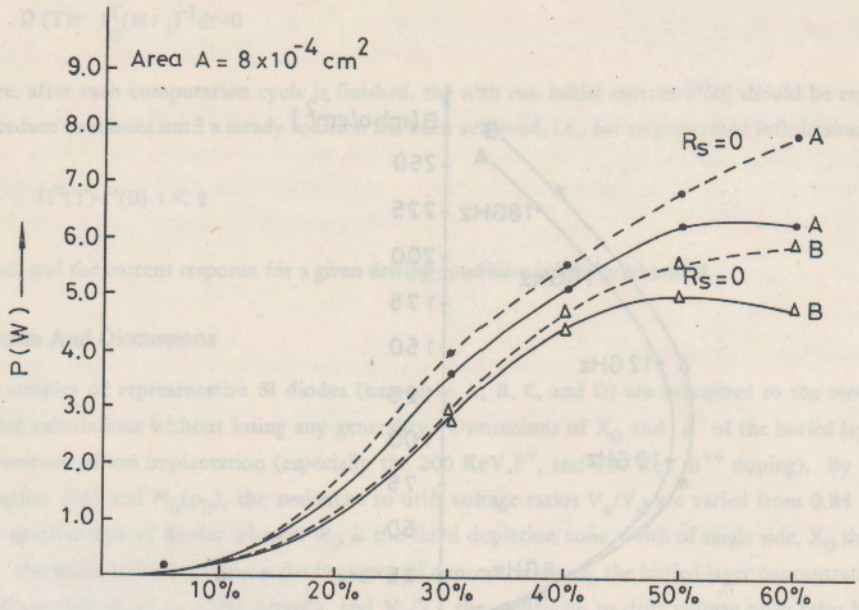

Fig. 4. Output power versus r.f. drive of diodes A and B. The solid-line shows data modified with the effect of moving zone edges, and the dashed line shows the unmodified results.

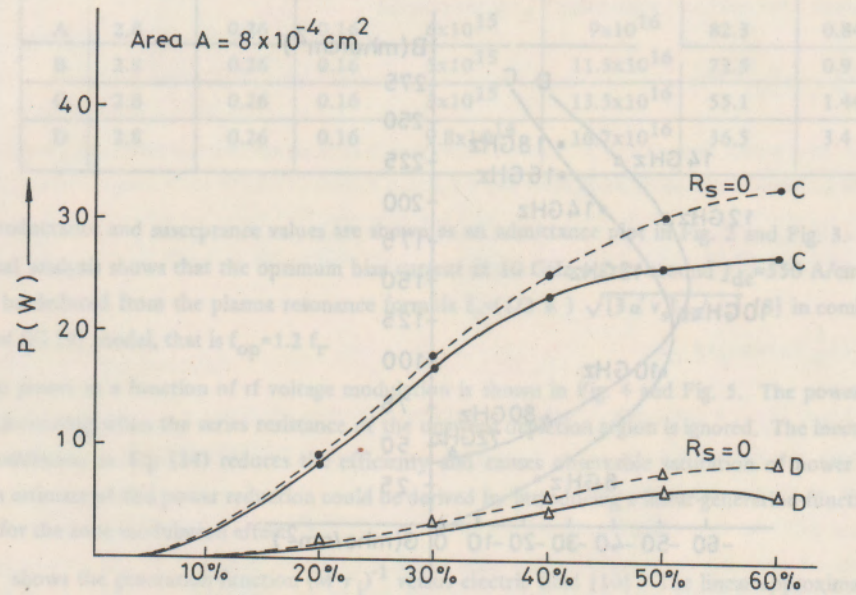

Fig. 5. Output power versus r.f. drive of diodes C and D. The dolid-line shows data modified with the effect of moving zone edges and the dashed-line shows the unmodified results.

it is clear that at $x=x_a$ where the peak generation occurs, the time integration of the second half period of the total field $E_t(t)$ should be equal to that of the first half period. Now, the amplitude of the perturbed field is flattened in the second half period as shown in Fig. 7(b) and expressed by Eq. (30). The induced space charge field will squeeze the first cycle, making a phase advance $\Delta\phi$ as shown in Fig. 7. The phase advance $\Delta\phi$ could be estimated by the

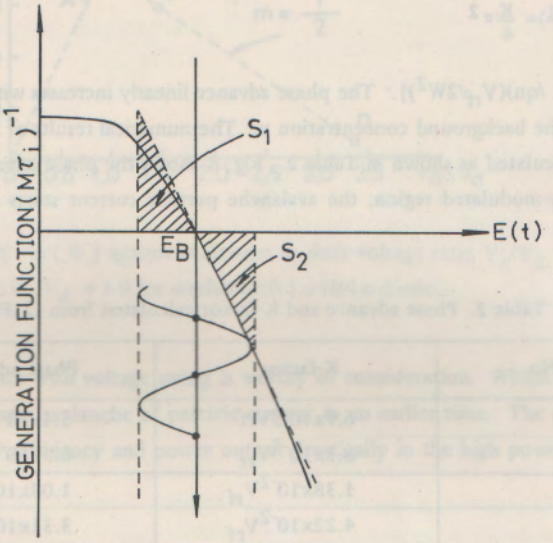

Fig. 6. A linear-generation-function model for calculating the avalanche current advance of $\Delta\phi$ in the presence of zone width modulation.

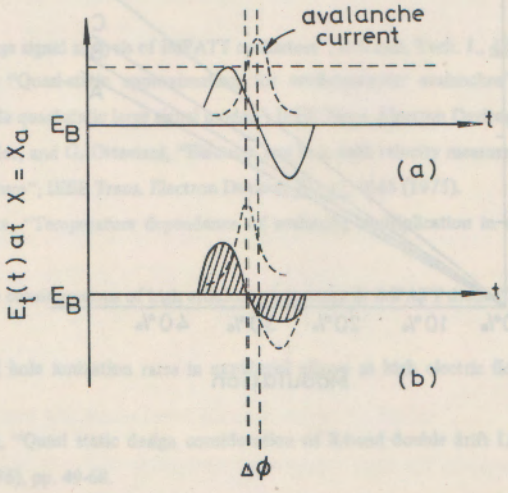

Fig. 7. (a) The perturbation $V_{rf}\sin\omega t$; (b) part of the second half of perturbation is droped in the unswept depletion zone. The phase advance $\Delta\phi$ is necessary for the condition $\int_0^T (M\tau_i)^{-1}dt=0$.

above mentioned equal area rule. Assuming a sinusoid with the same amplitude E_{rf} but with heigher frequency f_1, thus

$$\int_0^{T_1/2} E_{rf}\sin\omega_1 t\,dt = \left| \int_{T/2}^{T} E_{rf}\sin\omega t\,dt + \int_{T/2}^{T} E_{rf} K\sin^2\omega t\,dt \right| \tag{46}$$

and we obtain the phase advance

$$\Delta\phi = \pi\left(1-\frac{T_1}{T}\right) = \frac{K}{4}\pi^2 \tag{47}$$

where the factor $K=[(\epsilon_s/qn)(V_{rf}/2W^2)]$. The phase advance linearly increases with the swing voltage V_{rf}, but is inversely proportional to the background concentration n. The numerical results of K factor and phase advance $\Delta\phi$ as a function of V_{rf} are calculated as shown in Table 2. Fig. 8 shows the phase advance $\Delta\phi$ as a function of voltage modulation. In a highly-modulated region, the avalanche particle current starts earlier and causes degradation in power and efficiency.

Table 2. Phase advance and K-factor calculated from LGF model.

Diode No.	K-factor	Phase advance $\Delta\phi$
A	6.9x10-3Vrf	$5.4\times10^{-3}V_{rf}$
B	$8.3\times10^{-3}V_{rf}$	$6.5\times10^{-3}V_{rf}$
C	$1.38\times10^{-2}V_{rf}$	$1.08\times10^{-2}V_{rf}$
D	$4.22\times10^{-2}V_{rf}$	$3.31\times10^{-2}V_{rf}$

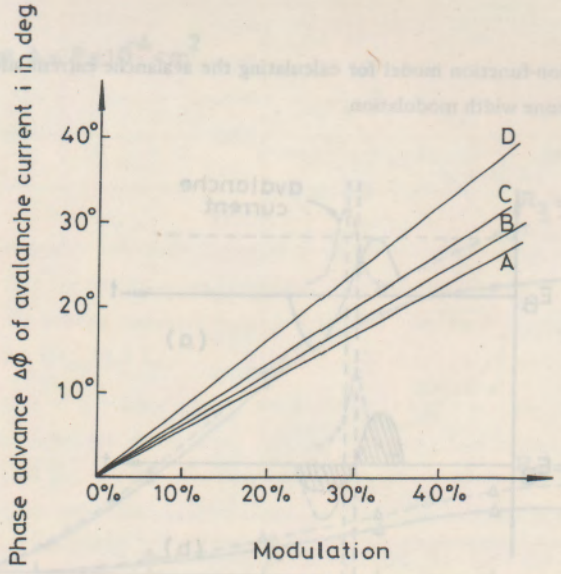

Fig. 8. Phase advance $\Delta\phi$ of avalanche current versus modulation percentage drived from the linear-generating function model.

The output power efficiency η (%) plotted against the avalanche-to-drift-voltage ratio V_a/V_d is shown in Fig. 9, for 50% modulation. The optimum efficiency η =18%, which is lower than the value η =21% predicted by the SG model, occurs around $V_a/V_d \approx 1.0$ for the double drift Lo-Hi-Lo Si diodes.

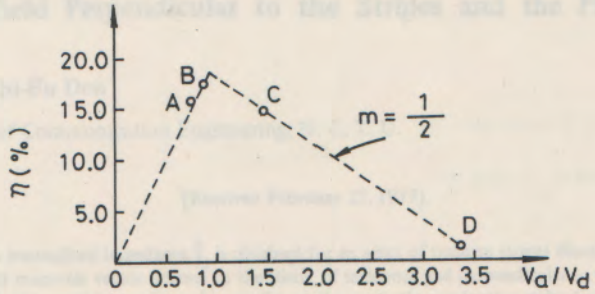

Fig. 9. Plot of efficiency η (%) against avalanche to drift voltage ratio V_a/V_d. Optimum condition appears at $V_a/V_d \approx 1.0$ for double-drift Lo-Hi-Lo diodes.

V. Conclusion

The variation of series resistance with voltage swing is worthy of consideration. Which causes power losses due to the undepleted material and starts avalanche of particle current in an earlier time. The premature fall-off of the electric field will degrade diode's efficiency and power output drastically in the high power double drift Read-like diodes and should not be ignored.

Acknowledgement

The authors wish to thank Mr. L. Chang for his cooperation in the program implementation and Mrs. M. C. Chang for help in arranging the manuscript. Thanks are also due to the staffs of the computer center of N. C. T. U. for their constant assistance.

References

1. J. L. Blue, "Approximate large signal analysis of IMPATT oscillators", Bell syst. Tech. J., 48, 383 (1969).
2. R. Kuvås and C. A. Lee, "Quasi-static approximation for semiconductor avalanches", J. Appl. Phys., 41, 1743 (1970).
3. D. R. Decker, "IMPATT diode quasi-static large signal model", IEEE Trans. Electron Devices, ED-21, 469 (1974).
4. C. Canali, G. Majni, R. Minder, and G. Ottaviani, "Electron and hole drift velocity measurements in Si and their empirical relation to electric field and temperature", IEEE Trans. Electron Devices, ED-22, 1045 (1975).
5. C. R. Crowell and S. M. Sze, "Temperature dependence of avalanche multiplication in semiconductors," Appl. Phys. Lett., 9, 242 (1966).
6. S. Su and S. M. Sze, "Design considerations of high efficiency low noise Si IMPATT diodes". IEEE Trans. Electron Devices, ED-20, 755 (1973).
7. W. N. Grant, "Electron and hole ionization rates in expitaxial silicon at high electric fields", Solid State Electronics, 16, 1189 (1973).
8. M. C. Chang & M. C. Chen, "Quasi static design consideration of X-band double drift Lo-Hi-Lo silicon IMPATT diodes", J. of N. C. T. U., Vol. 1, Dec. (1976), pp. 49-68.
9. D. L. Scharfetter and H. K. Gummel, "Large signal analysis of a silicon Read diode oscillator," IEEE Trans. Electron Devices, ED-16, No. 1, Jan. 64 (1969).
10. R. L. Juvås, "Nonlinear noise theory for IMPATT diodes," IEEE Trans. Electron Devices, ED-23, NO. 4, April, 395 (1976).